

# **Insights of many body degrees of freedom in (p,pN) reactions**

**Raquel Crespo**

Collaboration: E. Cravo, A. Deltuva, R.B. Wiringa, D. Jurčiukonis, M. Piarulli, A. Arriaga



**U LISBOA** | UNIVERSIDADE  
DE LISBOA

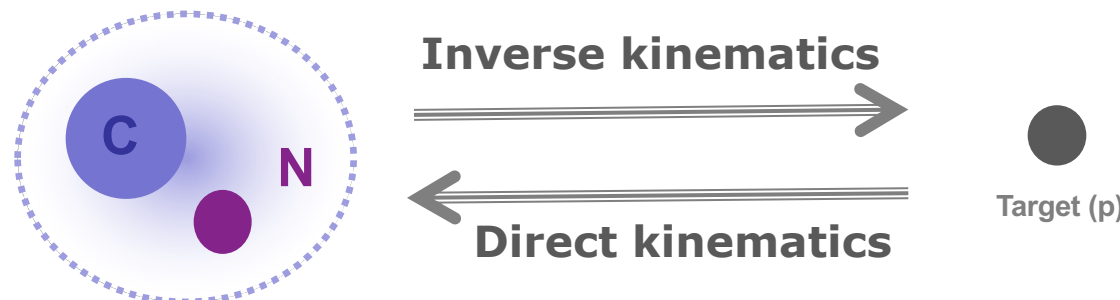


# Synopsis

- Motivation
- Revisit  ${}^A X(p,pN)$  at 400 MeV/u (inverse kinematics) for light nuclei
  - E. Cravo, R.B. Wiringa, R. Crespo, A. Arriaga, A. Deltuva and M. Piarulli
- Revisit  ${}^{12}C(p,2p)$  at 100 Mev/u (direct kinematics) measured at IUCF
  - A. Deltuva, E. Cravo, R. Crespo, D. Jurciukonis, submitted for publication
- Dynamical core excitation signatures in kinematical fully exclusive observables
  - E. Cravo, R. Crespo, A. Deltuva
- Perspectives

# Motivation

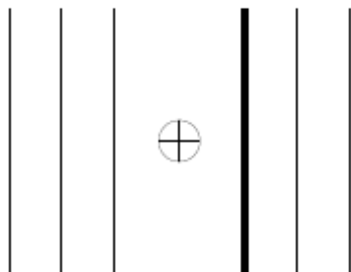
- Truncated Hilbert space



- Spectator core during the scattering process

One-nucleon **spectroscopic overlaps** (its strength being the **SF**) become the structure input to the reaction formalism.

$$\mathcal{H} = \mathcal{H}_g \oplus \mathcal{H}_x$$

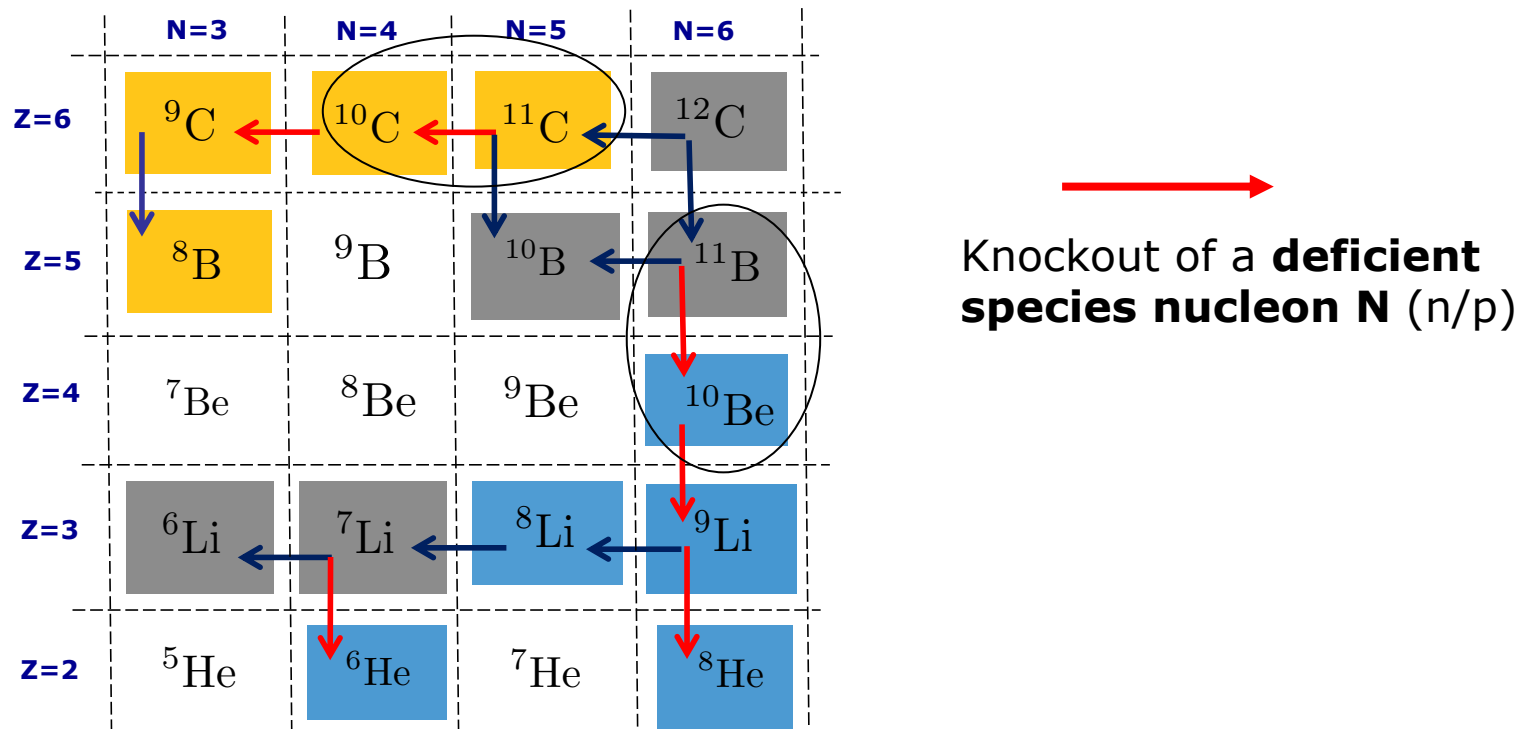


- 2-body DWIA =  $\mathcal{R} \times \text{PWIA}$
- 3-body Faddeev-AGS (F/AGS)
- 3-Body CDCC, TC,
- ...

# Motivation

- Can the *p*-shell spectroscopic quenching obtained from structure and reactions be conciliated ?
- Can observables for (p,pN) reactions provide unequivocal information about nuclear spectroscopy, testing structure models and their underlying interactions ?
- What is the role of many-body degrees of freedom ?

# Revisit ${}^A_X(p,pN)$ at 400 MeV/u (inverse kinematics)

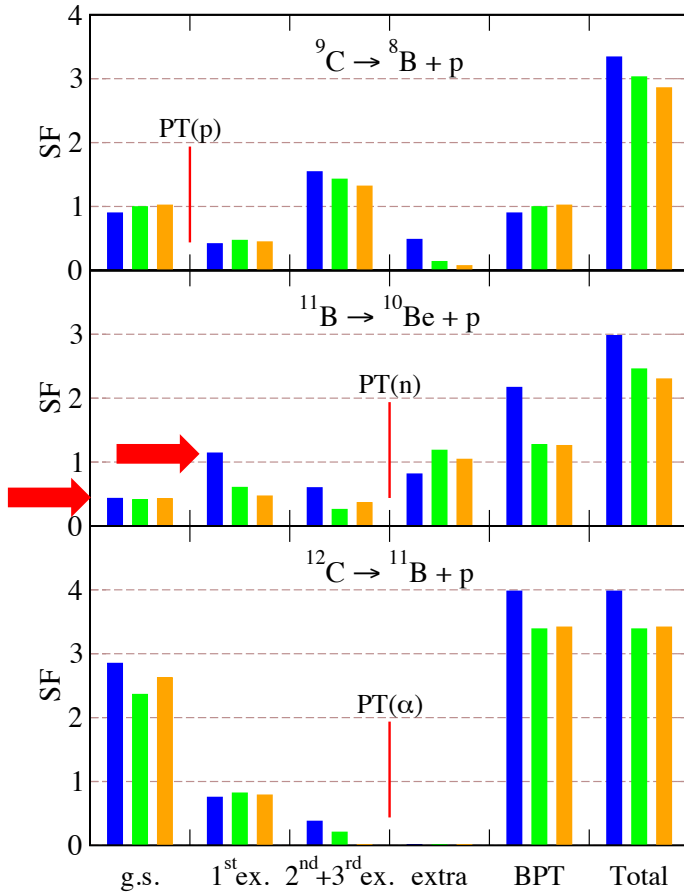
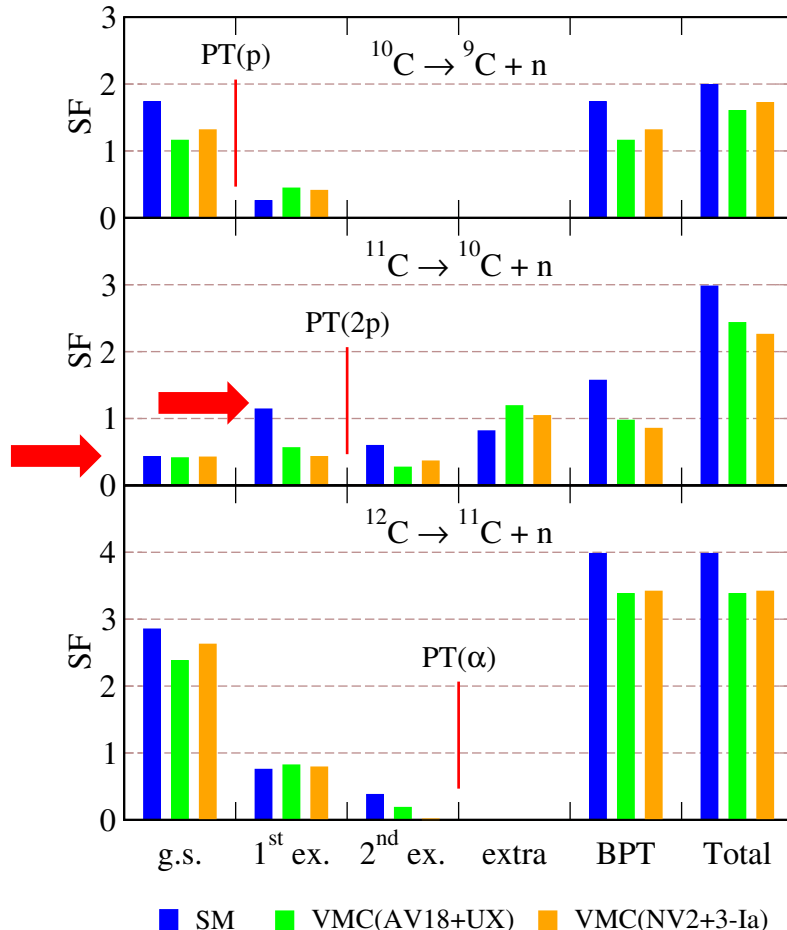


**Approach:** Merging into the **Fadd/AGS** reaction mechanism the SO overlaps deduced from **Quantum Monte Carlo Techniques (QMC)** using two interactions:

- Argonne V18 two-nucleon and Urbana X three-nucleon potentials (AV18+UX)
- Norfolk NV2+3  $\Delta$ -full local chiral field theory

# Revisit ${}^A X(p, pN)$ at 400 MeV/u (inverse kinematics)

Selected examples and **special cases in mirror transitions**

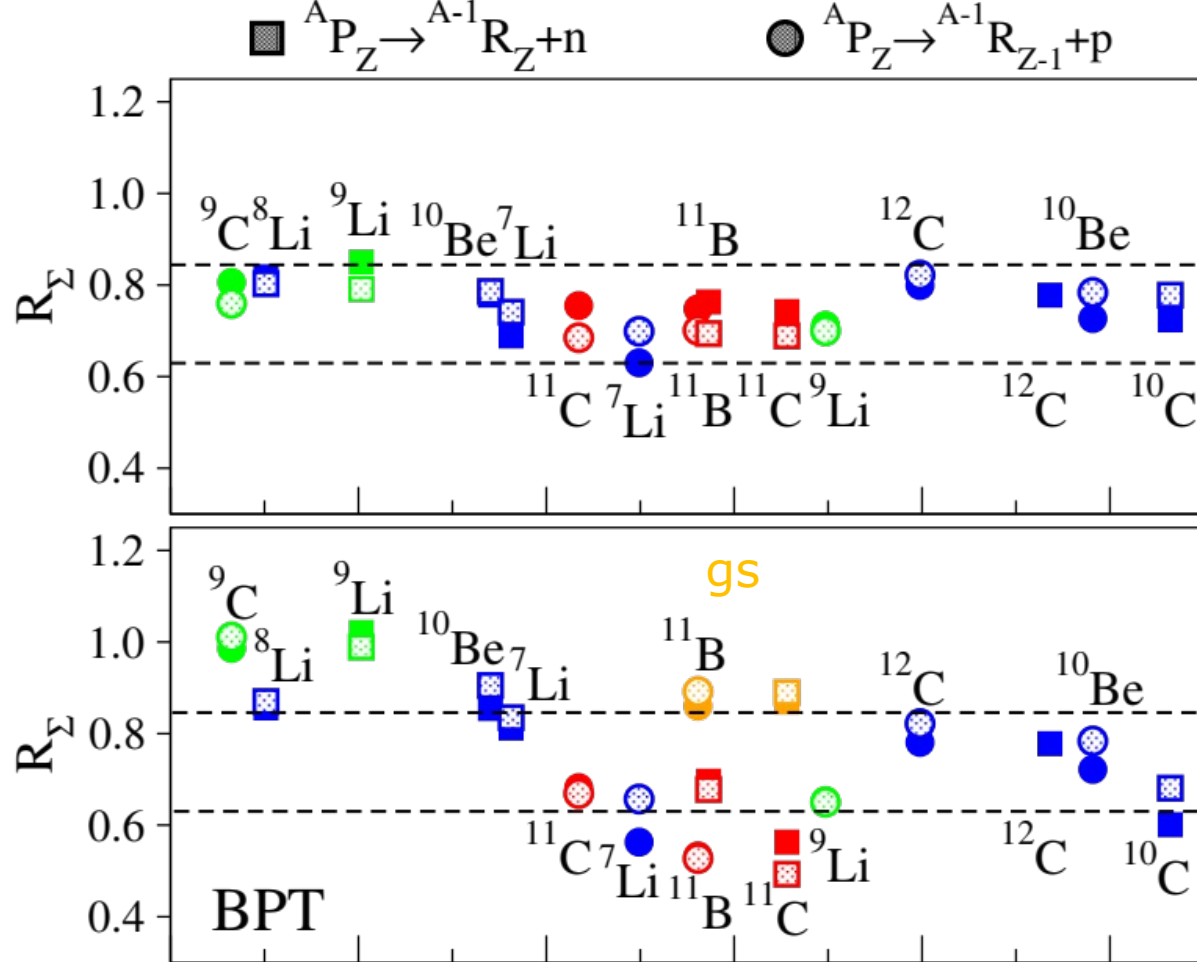


E.C., R.B.W., R.C., A.A., A.D. and M.P.

SFs and their sums – total and BPT

Raquel Crespo, DREB2024, Wiesbaden, 2024

# Revisit ${}^A\text{X}(\text{p},\text{pN})$ at 400 MeV/u (inverse kinematics)



$$\Sigma(\mathcal{M}) = \sum_i Z^i(\mathcal{M})$$

$$R_\Sigma = \frac{\Sigma(\text{QMC})}{\Sigma(\text{SM})}$$

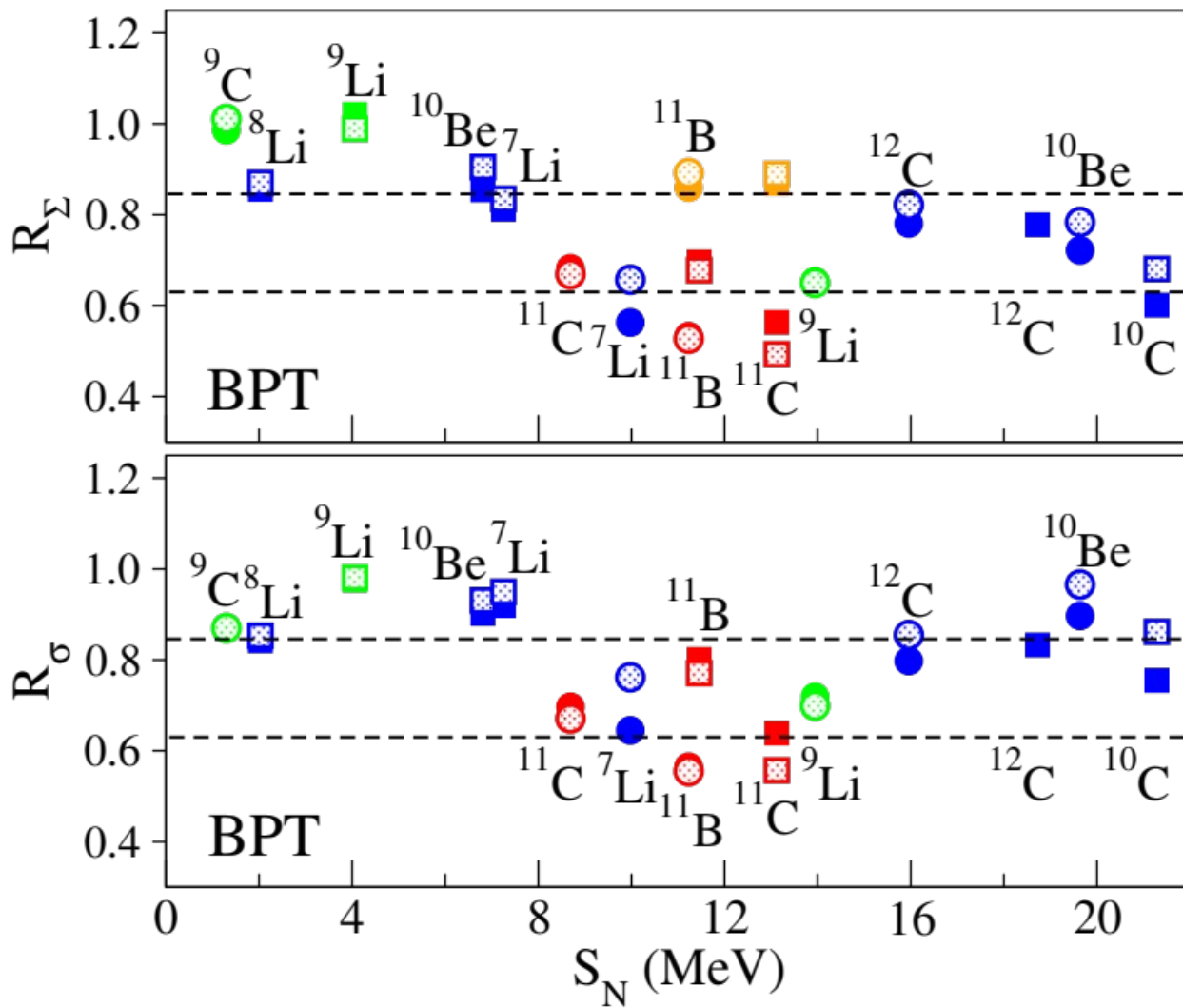
Total sums of SFs

$$R_\Sigma \sim 2/3$$

Sums of SFs that contains the states BPT

E.C., R.B.W., R.C., A.A., A.D. and M.P.

# Revisit ${}^A X(p, pN)$ at 400 MeV/u (inverse kinematics)



Sums of cross sections BPT, using the standard Faddeev/AGS reaction formalism

$$\sigma_{\text{th}}(\mathcal{M}) = \sum_i Z^i(\mathcal{M}) \sigma_{\text{sp}}^i(\mathcal{M})$$

$$R_{\sigma} = \frac{\sigma_{\text{th}}(\text{QMC})}{\sigma_{\text{th}}(\text{SM})}$$

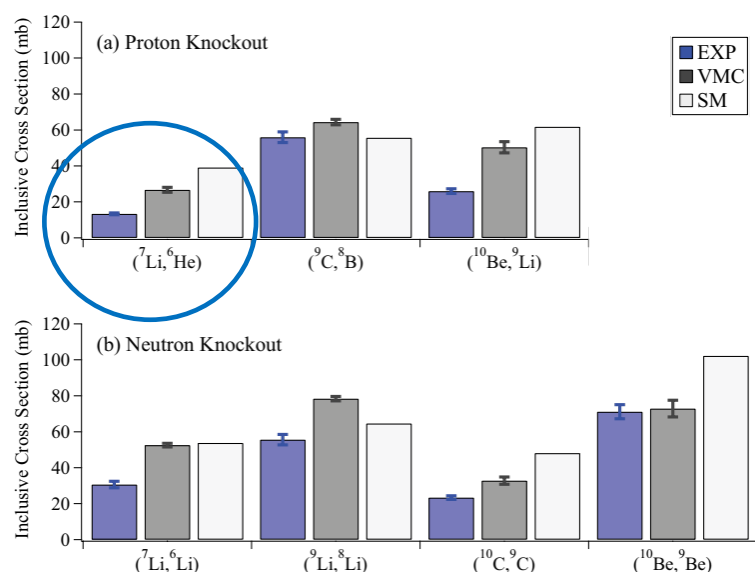
# Revisit ${}^A X(p, pN)$ at 400 MeV/u (inverse kinematics)

Reaction	QMC			SM	
	AV18-UX	NV2+3-Ia	NV2+3-Ia*/IIb*	CK	OXBASH [5] [10]
${}^{12}\text{C}(p, 2p){}^{11}\text{B}$	0.90	0.79	0.99/0.84	0.72	0.60(6)(4)
${}^{12}\text{C}(p, pn){}^{11}\text{C}$	1.08	--	--	0.90	0.80(9)(7)
${}^{11}\text{C}(p, 2p){}^{10}\text{B}$	1.34	1.52	--	0.92	0.86(4)(5)
${}^{11}\text{C}(p, pn){}^{10}\text{C}$	1.81	2.08	--	0.96	1.06(9)(12)
${}^{10}\text{C}(p, pn){}^9\text{C}$	1.43	1.23	--	1.08	0.99(13)(9)

$$R_S(\mathcal{M}) = \frac{\sigma_{\text{exp}}}{\sigma_{\text{th}}(\mathcal{M})}$$

The theoretical QMC cross sections **underestimates** the data for  $\sim$  factor 2 for  ${}^{11}\text{C}(p, pn)$

E.C., R.B.W., R.C., A.A., A.D. and M.P.



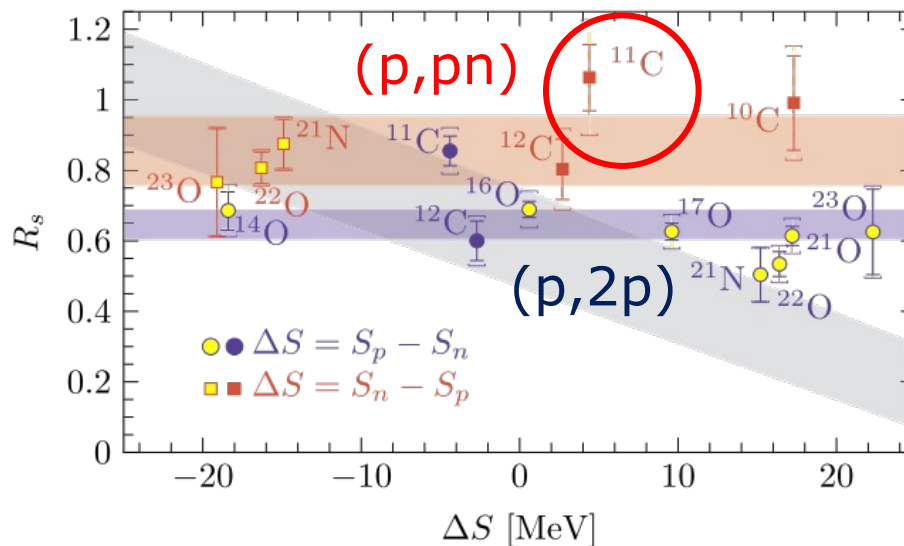
The theoretical QMC cross sections **overestimates** the data for  $\sim$  factor 2 for p removal from  ${}^7\text{Li}$

G.F. Grinyer, D. Bazin, A. Gade, J.A. Tostevin et al, Pys Rev C 86, 024315 (2012)

# Revisit ${}^A X(p, pN)$ at 400 MeV/u (inverse kinematics)

$$R_S(\mathcal{M}) = \frac{\sigma_{\text{exp}}}{\sigma_{\text{th}}(\mathcal{M})}$$

Reaction	QMC			SM	
	AV18-UX	NV2+3-Ia	NV2+3-Ia*/IIb*	CK	OXBASH [5, 10]
${}^{12}\text{C}(p, 2p){}^{11}\text{B}$	0.90	0.79	0.99/0.84	0.72	0.60(6)(4)
${}^{12}\text{C}(p, pn){}^{11}\text{C}$	1.08	--	--	0.90	0.80(9)(7)
${}^{11}\text{C}(p, 2p){}^{10}\text{B}$	1.34	1.52	--	0.92	0.86(4)(5)
${}^{11}\text{C}(p, pn){}^{10}\text{C}$	1.81	2.08	--	0.96	1.06(9)(12)
${}^{10}\text{C}(p, pn){}^9\text{C}$	1.43	1.23	--	1.08	0.99(13)(9)

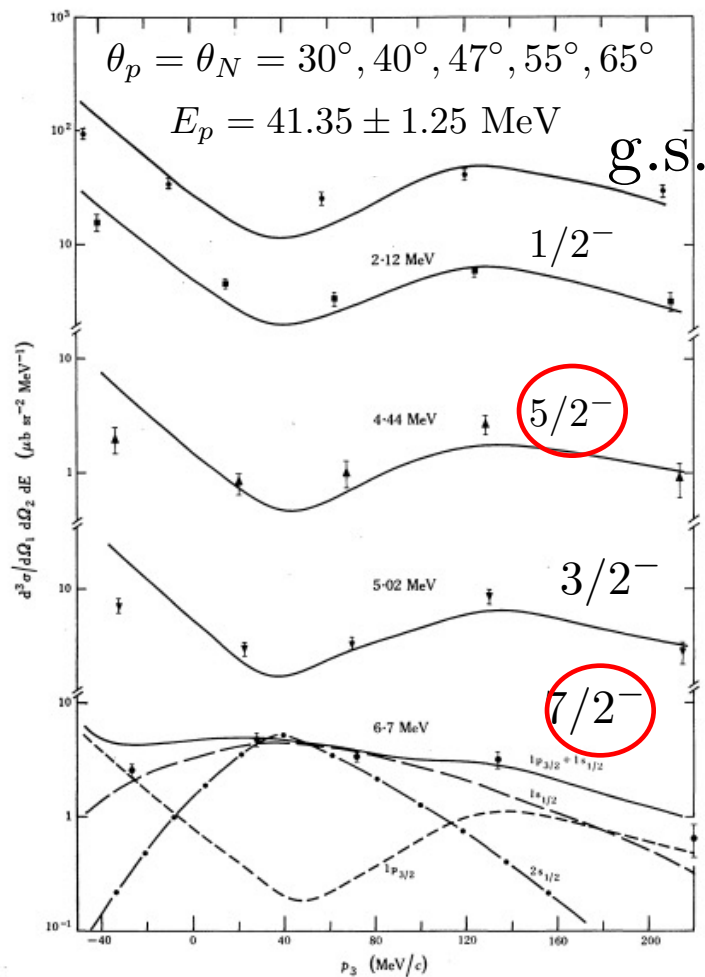


DWIA + SM-OXBH ~1

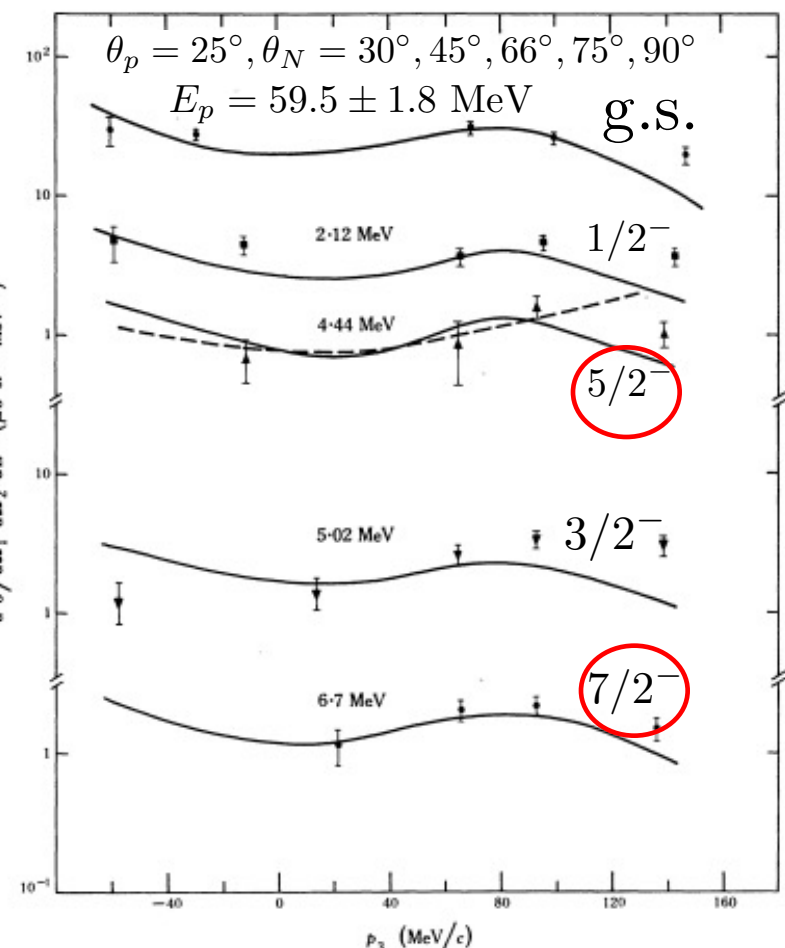
M. Holl, V. Panin, H. Alvarez-Pol,  
L. Atar, T. Aumann et al, Phys  
Lett B 795 (2019), 682

# Revisit $^{12}\text{C}(\text{p},2\text{p})$ at 100 MeV/u (direct kinematics)

Geometry: coplanar, Symmetric



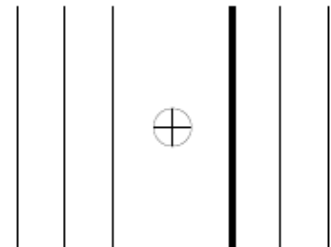
Geometry: coplanar, Asymmetric



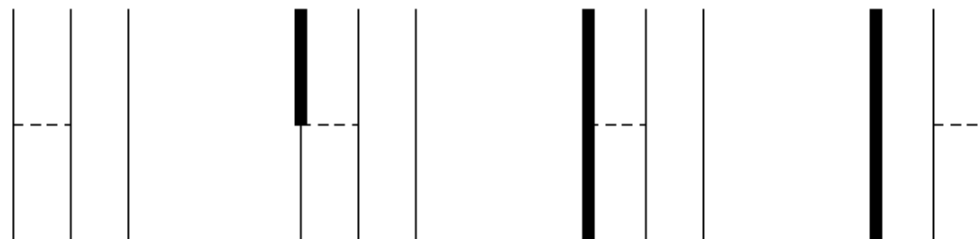
Devins et al, Aust. J. Phys 32, 323 (1979)

# Revisit $^{12}\text{C}(\text{p},2\text{p})$ at 100 MeV/u (direct kinematics)

$$\mathcal{H} = \mathcal{H}_g \oplus \mathcal{H}_x$$



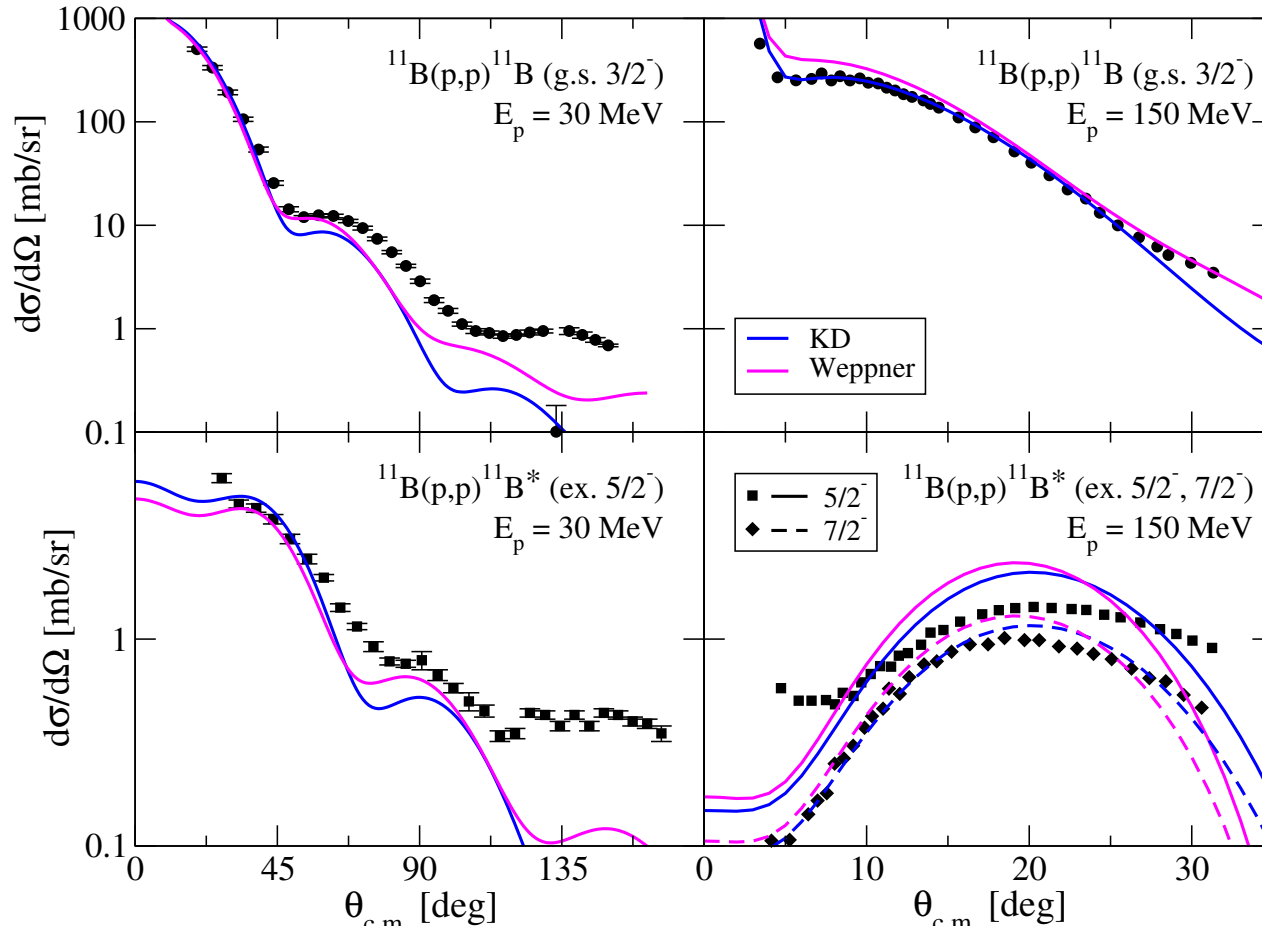
sector coupling by interaction



**The two sectors are coupled by the core – valence nucleon interaction**

A. Deltuva, PRC 88, 011601 (R) & [A. Deltuva talk](#)

# Revisit $^{12}\text{C}(\text{p},2\text{p})$ at 100 MeV/u (direct kinematics)



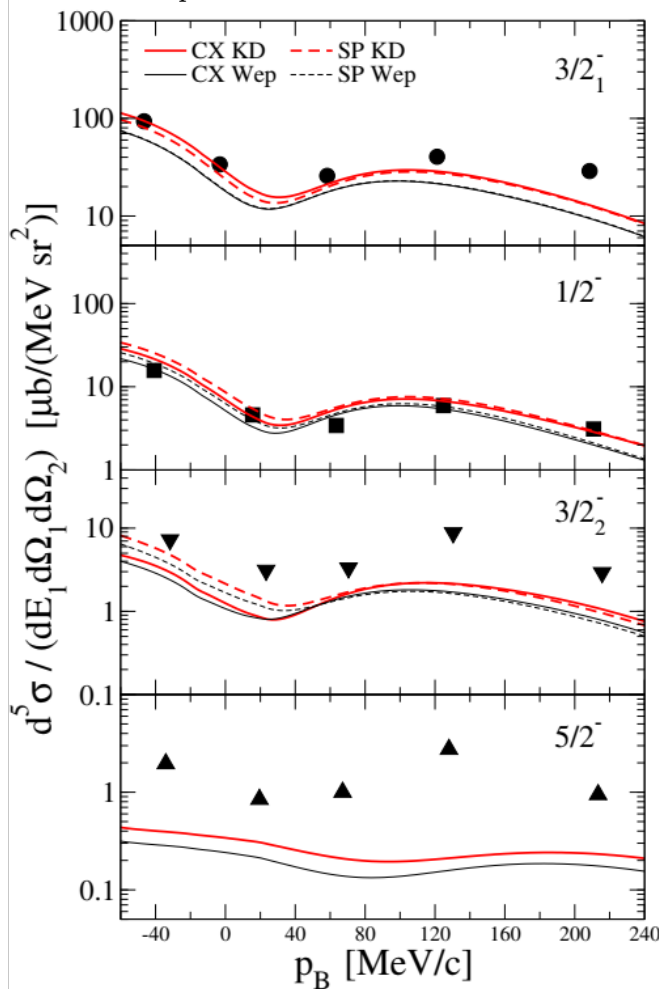
➤ Data: V.M. Hannen *et al*, Phys Rev C67, 054320 (2003)

A.D., E.C., R.C., D.J.

# Revisit $^{12}\text{C}(\text{p},2\text{p})$ at 100 MeV/u (direct kinematics)

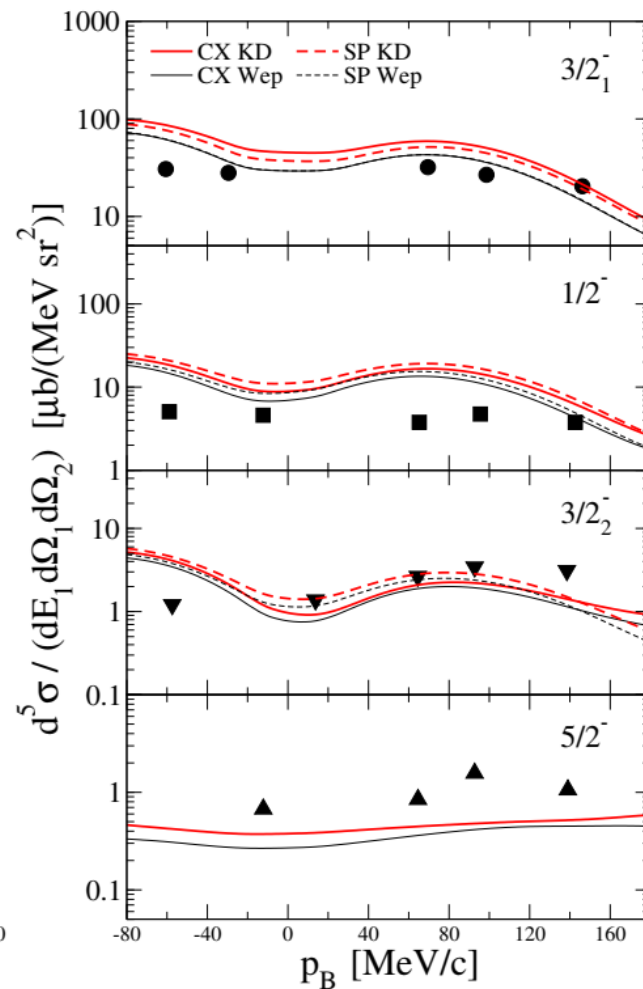
$$\theta_p = \theta_N = 30^\circ, 40^\circ, 47^\circ, 55^\circ, 65^\circ$$

$$E_p = 41.35 \pm 1.25 \text{ MeV}$$



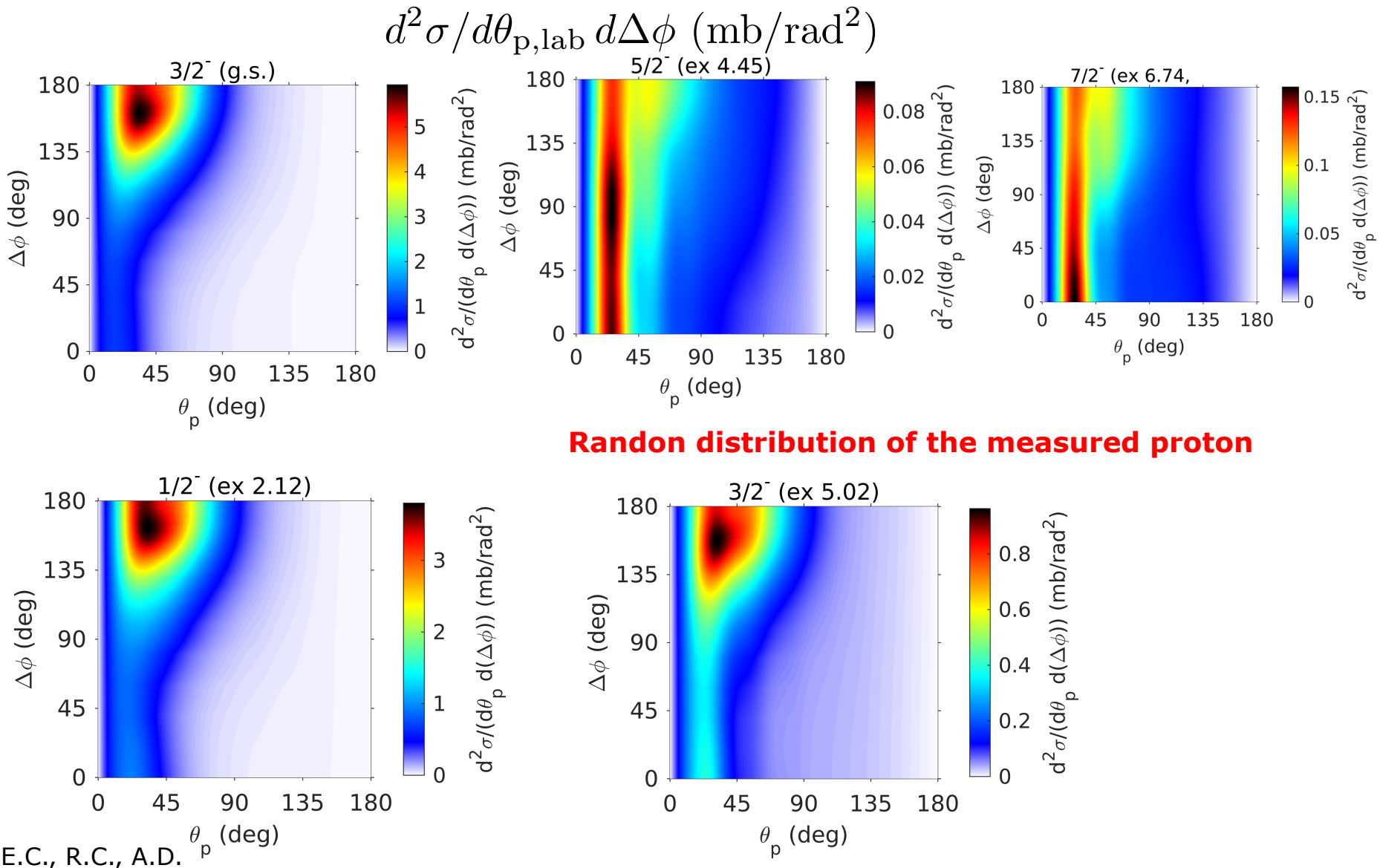
$$\theta_p = 25^\circ, \theta_N = 30^\circ, 45^\circ, 66^\circ, 75^\circ, 90^\circ$$

$$E_p = 59.5 \pm 1.8 \text{ MeV}$$



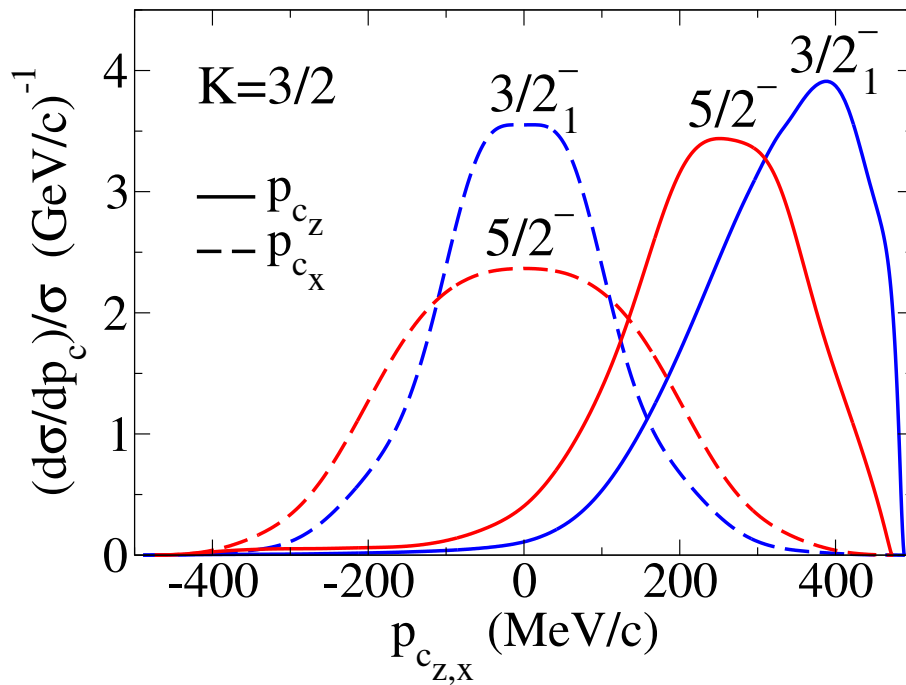
A.D., E.C., R.C., D.J.

# Dynamical core excitation signatures



# Dynamical core excitation signatures

Renormalized core momentum distributions for comparison

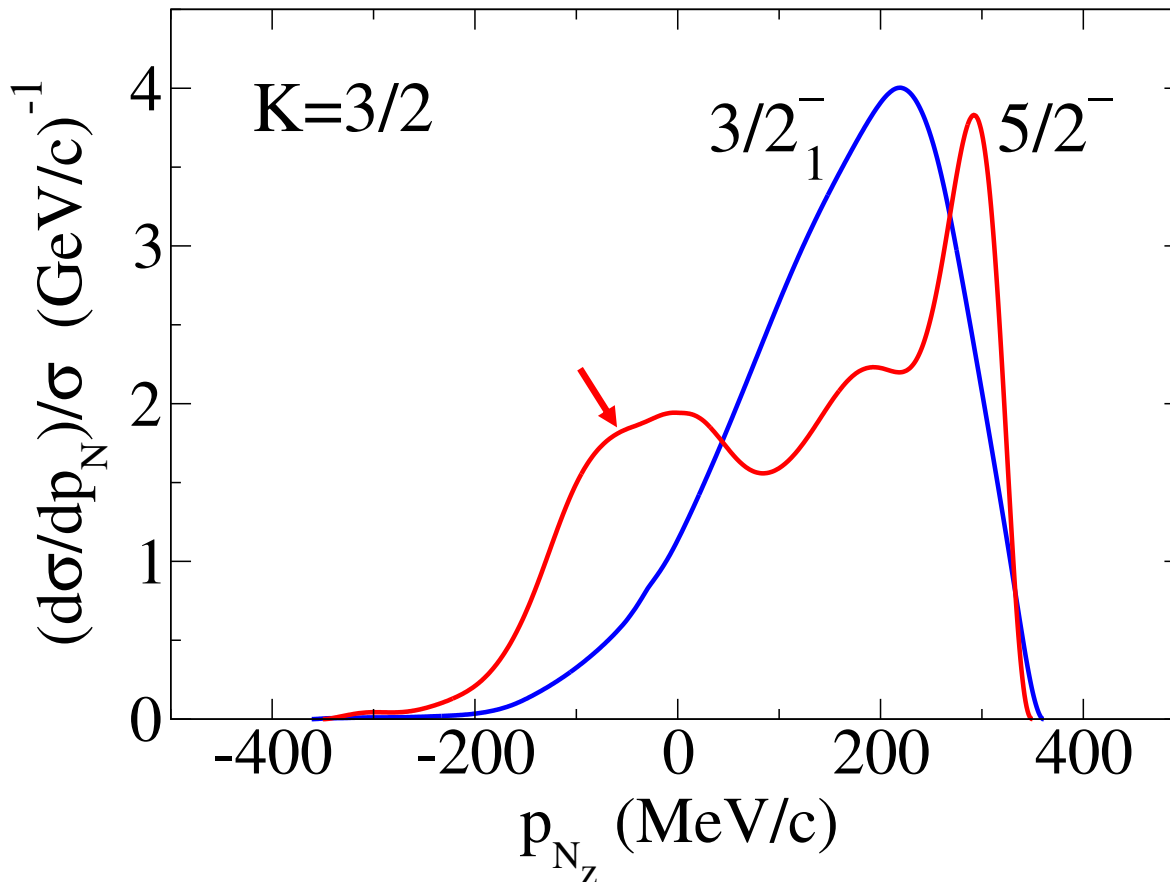


## Signature of core excitation:

- The **longitudinal core** momentum distribution **peaks at lower momentum**
- The **transverse core** momentum distribution is **broader**

E.C., R.C., A.D.

## Dynamical core excitation signatures

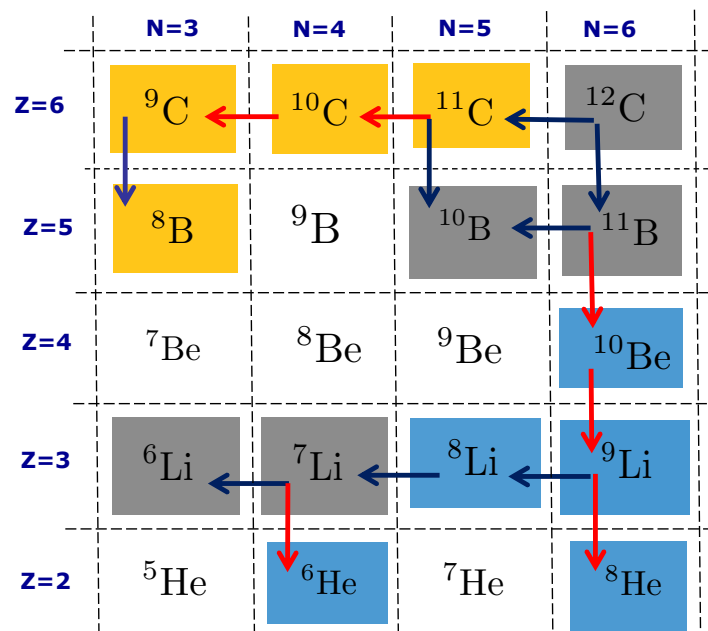


**Clear signature of core excitation:**

The longitudinal nucleon momentum distribution has a **double peak structure**

E.C., R.C., A.D.

# Perspectives



**Comprehensive theoretical & experimental program of  
N- knockout with light nuclei ( $A \leq 12$ )**

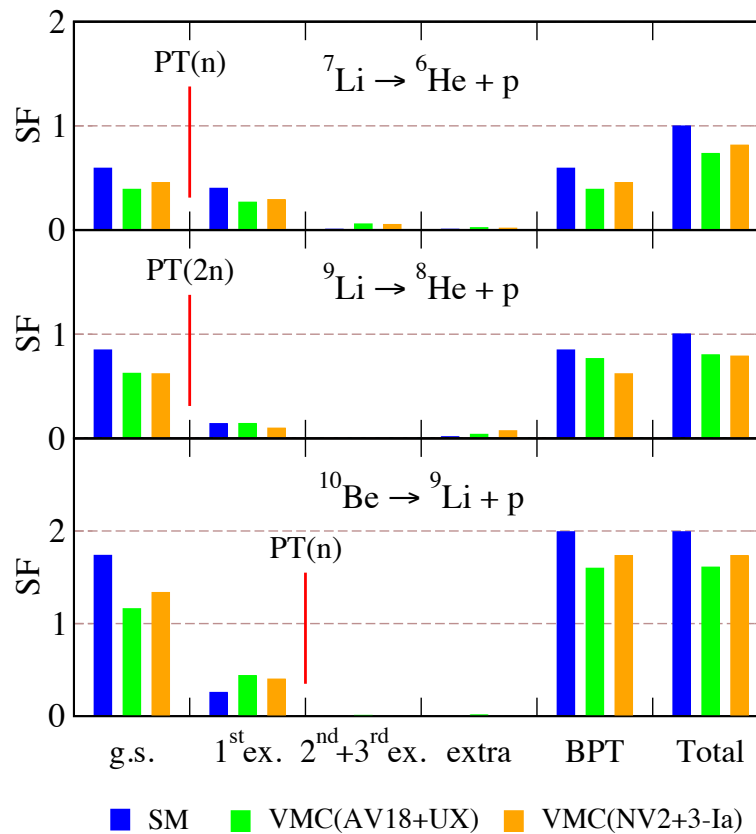
**Thank you !**

# Extra

Extra slides

# Revisit ${}^A X(p, pN)$ at 400 MeV/u (inverse kinematics)

Selected examples and **special cases in mirror transitions**

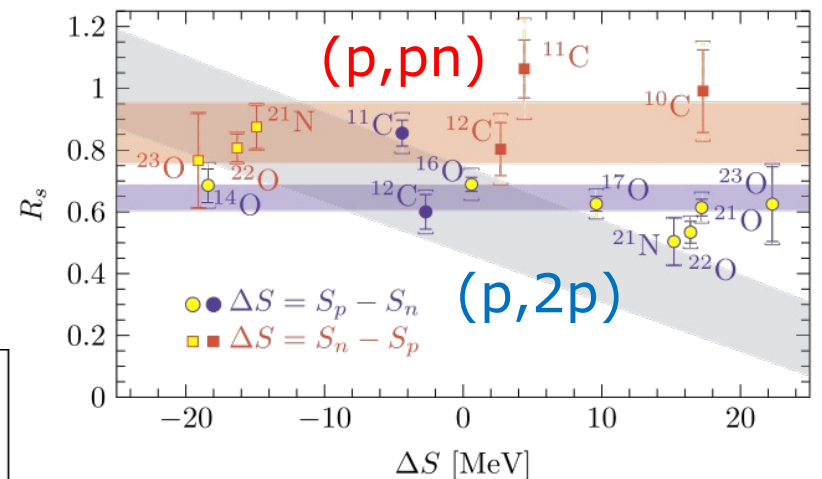
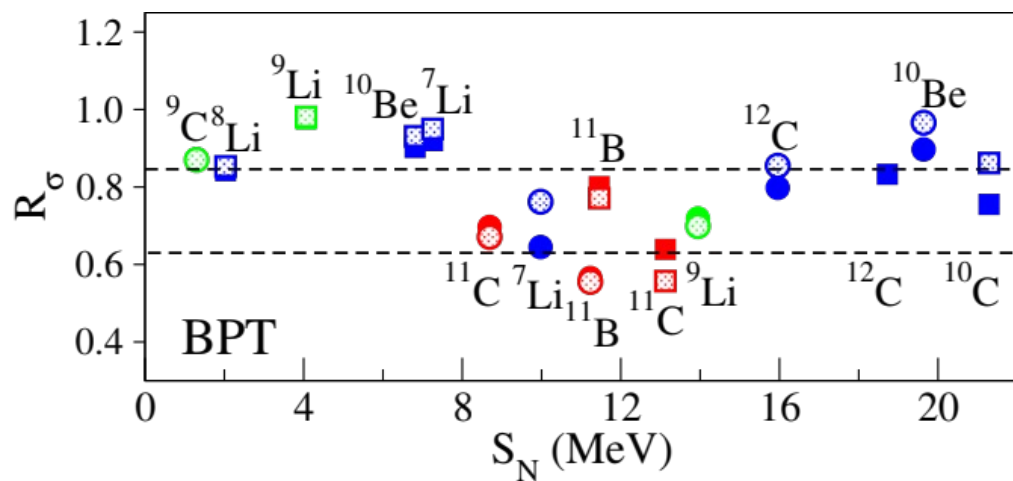


E.C., R.B.W., R.C., A.A., A.D. and M.P.

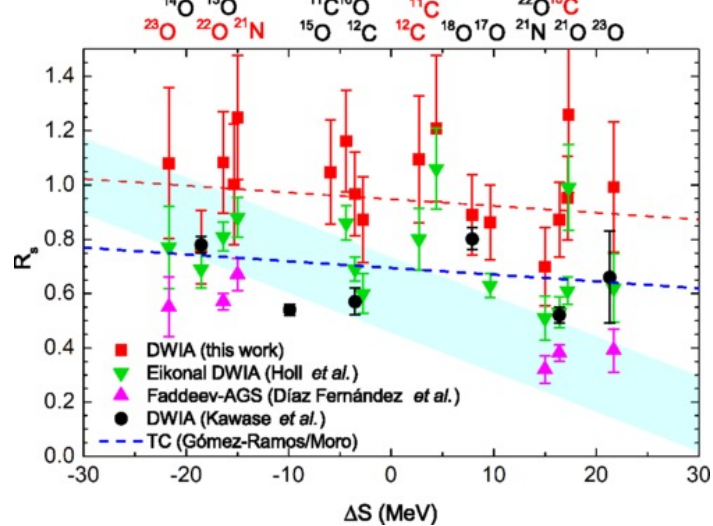
# Revisit ${}^A X(p, pN)$ at 400 MeV/u (inverse kinematics)

$\blacksquare {}^A P_Z \rightarrow {}^{A-1} R_{Z-1} + n$

$\bullet {}^A P_Z \rightarrow {}^{A-1} R_{Z-1} + p$



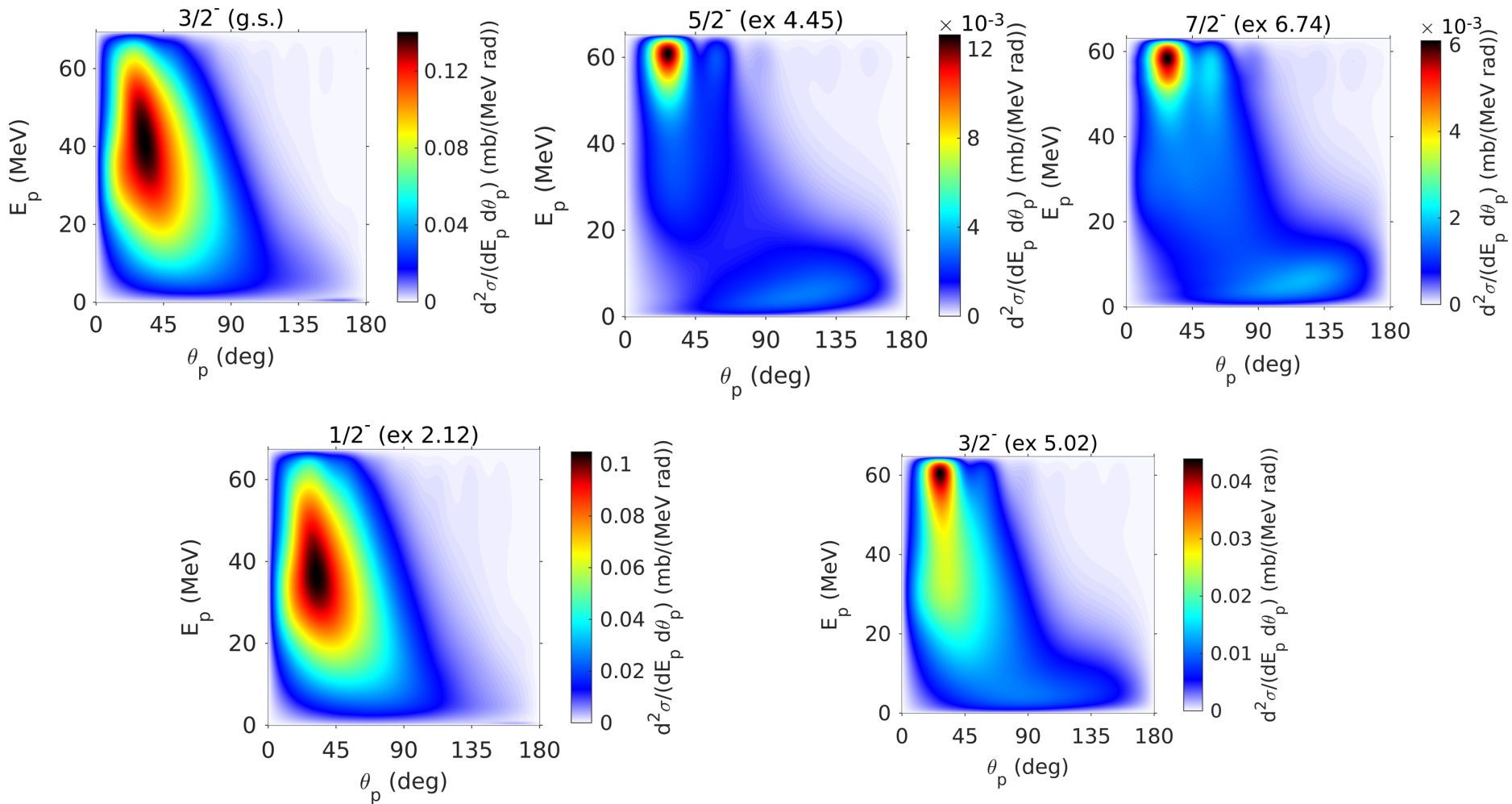
M. Holl, V. Panin, H. Alvarez-Pol, L. Atar, T. Aumann et al, Phys Lett B 795 (2019), 682



Nguyen Tr Toan Phuc, K. Yoshida, K. Ogata, Phys Rev C100, 064604

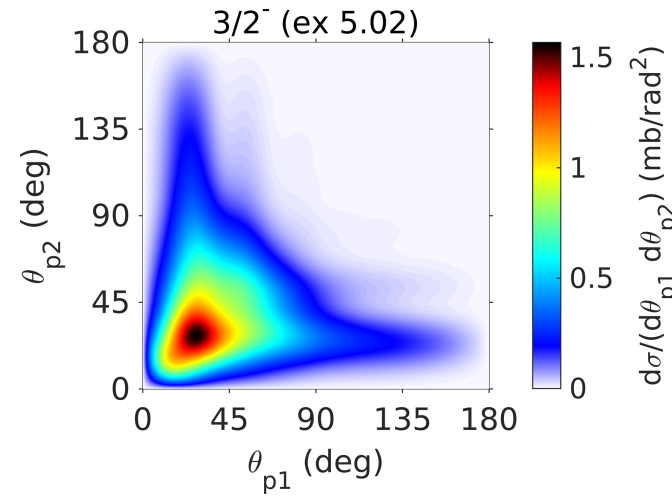
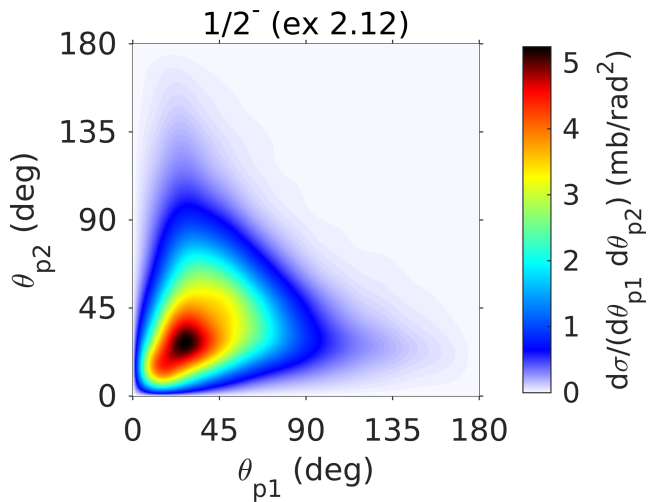
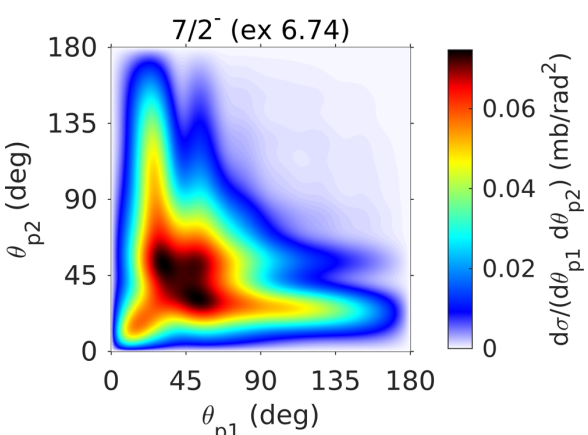
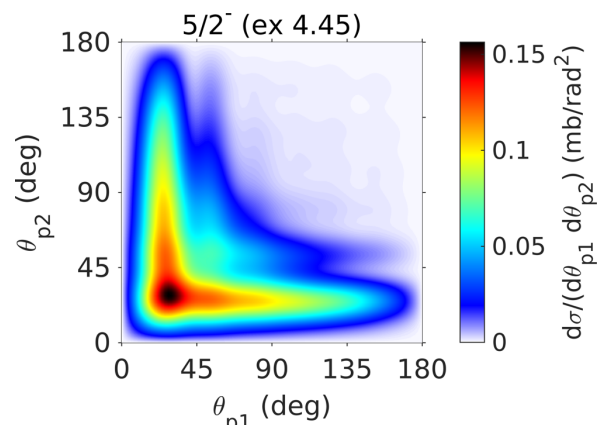
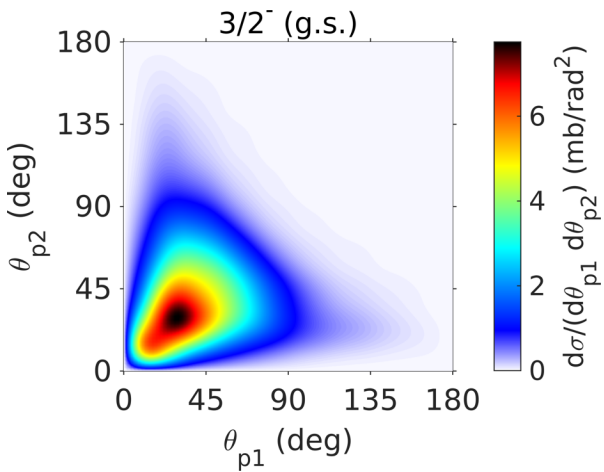
# Dynamical core excitation signatures

$d^2\sigma/dE_{p,\text{cm}}d\theta_{p,\text{cm}}$  (mb/MeV rad)



E.C., R.C., A.D.

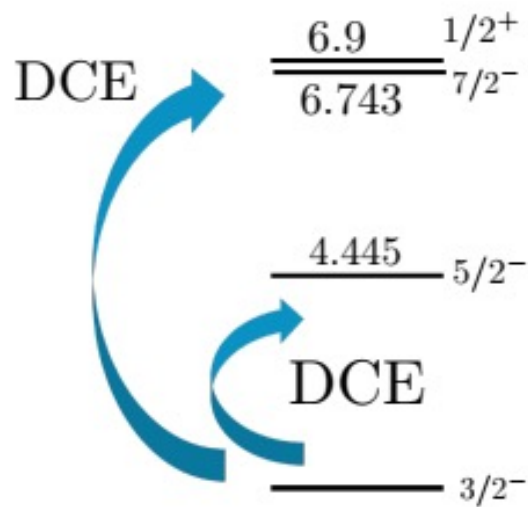
# Dynamical core excitation signatures



E.C., R.C., A.D.

# Revisit $^{12}\text{C}(\text{p},2\text{p})$ at 100 MeV/u (direct kinematics)

Two independent dynamical coupling problems for the scattering process



$$K = 3/2 \quad (\text{I})$$



$$K = 1/2$$

(II)

$$(\text{I}) \quad |\Phi^{JM}(^{12}\text{C}) > \simeq \alpha |3/2_1^- \otimes p_{3/2}(\pi) >$$

$$(\text{II}) \quad |\Phi^{JM}(^{12}\text{C}) > = \beta |1/2^- \otimes p_{3/2}(\pi) > + \gamma |3/2_2^- \otimes p_{3/2}(\pi) >$$

# Motivation

Geometry: coplanar, Symmetric

$$\theta_p = \theta_N = 30^\circ, 40^\circ, 47^\circ, 55^\circ, 65^\circ$$

$$E_p = 41.35 \pm 1.25 \text{ MeV}$$

Geometry: coplanar, Asymmetric

$$\theta_p = 25^\circ, \theta_N = 30^\circ, 45^\circ, 66^\circ, 75^\circ, 90^\circ$$

$$E_p = 59.5 \pm 1.8 \text{ MeV}$$

**Table 2. Spectroscopic factors obtained from DWIA calculations for  $^{11}\text{B}$  states populated in  $^{12}\text{C}(\text{p}, 2\text{p})^{11}\text{B}$**

State of $^{11}\text{B}$ $E_x$ (MeV)	$J^\pi$	Spectroscopic factors $C^2 S$			Theoretical results <sup>A</sup>		
		Symmetric	Asymmetric	CK	S	K	
g.s.	$3/2^-$	$2.0 \pm 0.2$	$1.0 \pm 0.2$	2.85	3.27	2.79	
2.12	$1/2^-$	$0.33 \pm 0.06$	$0.20 \pm 0.05$	0.38	0.60	0.79	
4.44	$5/2^-$	$0.10 \pm 0.05$	$0.11 \pm 0.04$	—	—	0.0005 <sup>B</sup>	
5.02	$3/2^-$	$0.33 \pm 0.1$	$0.13 \pm 0.03$	0.75	0.12	0.345	
6.74 <sup>C</sup>	$7/2^-$	$0.06 \pm 0.03$	$0.12 \pm 0.04$	—	—	0.035 <sup>B</sup>	
6.79 <sup>C</sup>	$1/2^+$	$0.05 \pm 0.02$					

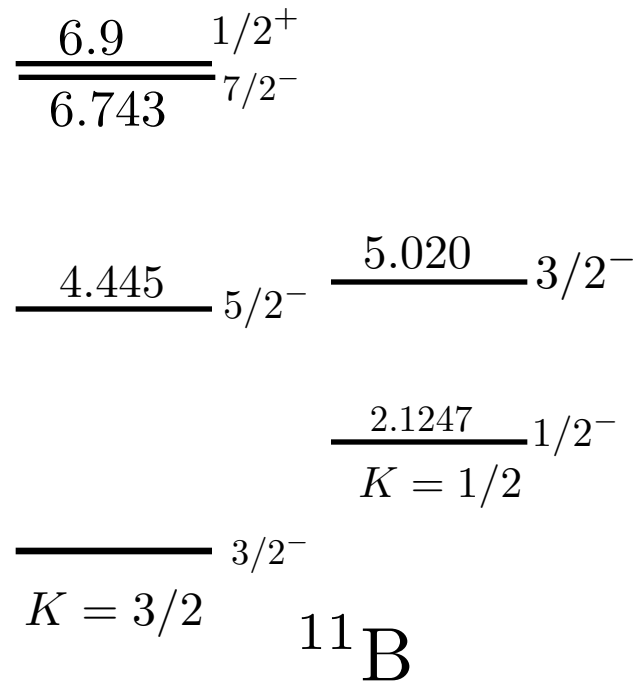
<sup>A</sup> Results from: CK, intermediate coupling calculation of Cohen and Kurath (1967); S, Singh *et al.* (1973); K, Kurath (1968).

<sup>B</sup> These calculations assumed f-wave knockout.

<sup>C</sup> These states were not resolved; see the text for the method of estimating their separate contributions.

Devins et al, Aust. J. Phys 32, 323 (1979)

# Motivation



$^{11}\text{B}$  is strongly deformed and the low lying states are of rotational nature:

The excitation spectra exhibit an approximate  $J(J+1)$  dependence

# Revisit $^{12}\text{C}(\text{p},2\text{p})$ at 100 MeV/u (direct kinematics)

$$U_{\beta\alpha} = \bar{\delta}_{\beta\alpha} G_0^{-1} + \sum_{\sigma} \bar{\delta}_{\beta\sigma} T_{\sigma} G_0 U_{\sigma\alpha}$$

$$U_{0\alpha} = G_0^{-1} + \sum_{\sigma} T_{\sigma} G_0 U_{\sigma\alpha}$$

$$\mathcal{H} = \mathcal{H}_g \oplus \mathcal{H}_x$$

$$T_{\sigma} = v_{\sigma} + v_{\sigma} G_0 T_{\sigma} \quad \text{2-particle Transition operator}$$

$$G_0 = (E + i0 - H_0)^{-1} \quad \text{Free resolvent}$$

$$\text{channel states} \quad (E - H_0 - v_{\alpha}) |\phi_{\alpha}\rangle = 0$$

$$H_0 |\mathbf{p}_{\alpha} \mathbf{q}_{\alpha}\rangle_a = [p_{\alpha}^2/2\mu_{\alpha} + q_{\alpha}^2/2M_{\alpha} + (\textcolor{blue}{m_{A^*} - m_A}) \delta_{ax}] |\mathbf{p}_{\alpha} \mathbf{q}_{\alpha}\rangle_a$$

Where the extended free Hamiltonian  $H_0$  is the sum of the kinetic energy operator and the intrinsic operator of the core whose contribution is the mass difference relative to the  $\text{A}+\text{p}+\text{n}$  threshold

# Revisit $^{12}\text{C}(\text{p},2\text{p})$ at 100 MeV/u (direct kinematics)

2-particle transition operator, requires the  
potentials  $v_\sigma$  for each interaction pair

$$T_\sigma = v_\sigma + v_\sigma G_0 T_\sigma$$

- Realistic CD BONN for the np interaction
- **N-Core** and **p-Core** interactions are obtained from a **rotation model for the core with a permanent quadrupole deformation.**  
In the body-fixed frame, the surface radius is parametrized as

$$R(\hat{\xi}) = R_0[1 + \beta_2 Y_{20}(\hat{\xi})]$$

**Input parameter: deformation lenght**

# Revisit $^{12}\text{C}(\text{p},2\text{p})$ at 100 MeV/u (direct kinematics)

Deformed surface radius

$$R(\hat{\xi}) = R_0[1 + \beta_2 Y_{20}(\hat{\xi})]$$

The N-Core and p-Core interactions are obtained assuming that the interaction follows the deformation of the Core.

That is: starting from a central potential,  $V_{xc}^{(0)}(r)$   
the X-core ( $x=\text{N,p}$ ) interaction is obtained by **deforming this central interaction**

$$V_{xc}(r, \hat{\xi}) = V_{xc}^{(0)}(r) \left[ r - \delta_2 Y_{20}(\hat{\xi}) \right] ; \quad \delta_2 = \beta_2 R_0$$

The deformed central interaction is supplemented by a central/deformed spin-orbit term

**Input parameter: deformation lenght**

$$\delta_2 = 1.5 \text{ fm}$$